

Inhibition of glioma by adenovirus KGHV500 encoding anti-p21Ras scFv and carried by cytokine-induced killer cells

Jing Qian^{1,2,3,*}, Mo Yang^{3,*}, Qiang Feng³, Xin-Yan Pan³, Li-Lin Yang³ and Ju-Lun Yang³ 

¹Faculty of Life Science and Technology, Kunming University of Science and Technology, Kunming 650500, PR China; ²Medical School, Kunming University of Science and Technology, Kunming 650500, PR China; ³Department of Pathology, 920th Hospital of the Joint Logistics Support Force of PLA, Kunming 650032, PR China

Corresponding author: Ju-Lun Yang. Email: yangjulun@sina.com

*These authors contributed equally to this work.

Impact statement

For glioma treatment, gene therapy/virotherapy approach is a promising candidate. The Ras gene is reported to play a vital role in the RAS/RAF/mitogen-activated protein kinase (MAPK) pathway in gliomas. Thus, targeting the Ras gene should be a reasonable potential therapeutic method for glioma. In the present study, we used cytokine-induced killer (CIK) cells as secondary vectors to systemically deliver recombinant adenovirus KGHV500 to glioma xenografts and investigated the anti-tumor efficiency of recombinant adenovirus KGHV500 *in vitro* and *in vivo*. Our results expand evidence that targeting Ras is a useful and potential therapeutic strategy for gliomas. We believe that anti-p21Ras scFv delivered by recombinant adenovirus and CIK cells may play an important role in the therapy of Ras-driven cancers.

Abstract

Ras gene mutation or overexpression can lead to tumorigenesis in multiple kinds of cancer, including glioma. However, no drugs targeting Ras or its expression products have been approved for clinical application thus far. Adenoviral gene therapy is a promising method for the treatment of glioma. In this study, the human glioma cell line U251 was co-cultured with recombinant adenovirus KGHV500, and the anti-tumor effects of KGHV500 were determined by MTT, scratch test, Transwell invasion, and apoptosis assays. Then, KGHV500 was delivered via the intravenous injection of CIK cells into glioma xenografts. Tumor volume, ki67 proliferation index, apoptosis levels, and anti-p21Ras scFv expression were tested to evaluate targeting ability, anti-tumor efficacy, and safety. We found that the KGHV500 exhibited anti-tumor activity in U251 cells and increased the intracellular expression of anti-p21Ras scFv compared with that in the control groups. CIK cells delivered KGHV500 to U251 glioma cell xenografts and enhanced anti-tumor activity against glioma xenografts compared to that produced by the control treatment. In conclusion, targeting Ras is a useful therapeutic strategy for gliomas and other Ras-driven cancers, and the delivery of anti-p21Ras scFv by recombinant adenovirus and CIK cells may play an essential role in the therapy of Ras-driven cancers.

Keywords: Glioma, anti-p21Ras scFv, recombinant adenovirus, CIK cells, gene therapy

Experimental Biology and Medicine 2021; 246: 1228–1238. DOI: 10.1177/1535370220986769

Introduction

Gliomas are the most common type of human tumors affecting the central nervous system (CNS), with almost 250,000 cases reported annually worldwide.¹ Currently, although there are multiple therapies available, such as aggressive surgery resection, radiation or chemotherapy, the survival rate of the patients remains poor.² Therefore, it is important to investigate novel and more specific therapies to address this tumor.

Ras genes (H-Ras, N-Ras, and K-Ras) encode proteins comprising 188–189 amino acids, known as p21 proteins, that cycle between a GTP-bound active form and a GDP-bound inactive form.³ These small GTP-binding proteins play a critical role in many signaling networks through

which cell proliferation, differentiation, migration, apoptosis, and senescence are regulated.⁴ Ras gene mutation or overexpression can lead to tumorigenesis in multiple kinds of cancer. The increased expression of Ras in glioma is first reported by Gerosa.⁵ Transcriptional regulation of Ras is positively correlated with the degree of glioma malignancy.⁶ In high-grade gliomas, although somatic Ras mutations are less common, they do express a high level of Ras protein as a consequence of the excessive activity of upstream ligands/receptors, such as EGFR.^{7,8} The activation of downstream signaling pathways, such as the classic RTK/RAS/PI3K signaling axis, which is altered in 88% of adult human gliomas, follows Ras activation.⁹ Therefore, the Ras gene may be an important

therapeutic target for gliomas. Up to now, no drugs targeting Ras or its expression products have been approved for clinical application.

Previously, we constructed recombinant adenovirus KGHV500, which carries the anti-p21ras single-chain antibody gene and can conditionally replicate and proliferate in tumor cells and expresses the anti-p21Ras single-chain antibody. KGHV500 demonstrated significant anti-tumor effects in lung cancer,¹⁰ colorectal cancer,¹¹ and in gastric cancer.¹² In this study, we employed CIK cells as secondary vectors to systemically deliver recombinant adenovirus KGHV500 to treat glioblastoma xenografts and investigated its anti-tumor efficiency and safety *in vitro* and *in vivo*.

Materials and methods

Cell lines and recombinant adenovirus

The human glioblastoma cell line U251 was obtained from the Cell Bank of the Chinese Academy of Science. The human embryonic kidney cell line HEK 293 was purchased from the Conservation Genetics CAS Kunming Cell Bank. All cells were cultured and supplemented with 10% fetal bovine serum (FBS) (Biological Industries, Israel), 100 units/mL penicillin, and 100 µg/mL streptomycin at 37°C with 5% CO₂.

The KGHV500 and KGHV400 adenoviruses were previously constructed from wild type adenovirus 5 by our laboratory. Both of them express the F35 fiber protein, which is the ligand of CD46. KGHV500 contains the anti-p21Ras scFv gene, but KGHV400 does not. The recombinant adenovirus was purified by discontinuous density gradient centrifugation with cesium chloride, and the viral titer was determined using the tissue culture infectious dose 50 (TCID₅₀) method¹³ in HEK 293 cells.

Detection of p21Ras and CD46 proteins in U251 cells

U251 cells were collected, fixed, paraffin embedded, and sectioned (Leica, R, Leica Company, Germany). Then, CD46 protein and p21H-ras were detected by immunohistochemistry (IHC) using an anti-CD46 monoclonal antibody (Abcam, EPR4014, UK) and anti p21Ras monoclonal antibody as the primary antibody, respectively.

Infection of U251 cells by the recombinant adenovirus

U251 cells at 1×10^6 cells/ml were seeded on six-well plates and grown to 70%–80% confluence, then were co-cultured with KGHV500 at various multiplicity of infection (MOI) values (50, 100, and 200) under conditions of 5% CO₂ at 37°C with saturated humidity to determine optimal MOI. After 48 h, KGHV500 infection in U251 cells was assessed with an inverted microscope (Nikon, Tokyo, Japan) and electron microscopy (EM) (JEM-1011, Japan).

Preparation and identification of CIK cells

Cytokine-induced killer (CIK) cells were generated from the peripheral blood mononuclear cells (PBMCs) of healthy donors, as previously described.¹⁴ The cell density was adjusted to 1×10^6 cells/ml in RPMI 1640 medium

(HyClone, Inc., USA) containing 10% FBS, and the cells were then cultured at 37°C with saturated humidity. On day 0, the cells were co-stimulated with IFN- γ (1000 U/ml, PeproTech, USA) for 24 h. On the second day, an anti-CD3 monoclonal antibody (50 ng/ml, OKT eBioscience, USA) and IL-2 (300 U/ml, PeproTech, USA) were added; fresh medium containing IL-2 was used to replace half of the old medium every three days until day 14. CIK cells were identified by immunohistochemistry with anti-CD3 monoclonal antibody (ZSGB-Bio, China) and anti-CD56 monoclonal antibody (MXB, China). IHC also detected CD46, the receptor for the KGHV500 fiber protein, on all CIK cells.

CIK cell infection with recombinant adenoviruses

CIK cells were co-cultured with KGHV500 at an MOI of 100. The hexon protein of adenovirus was detected in CIK cells by immunohistochemistry to determine the infection efficiency of KGHV500.

Scratch test to assess cell migration

U251 cells were seeded in 6-well plates and cultured overnight. A wound was made with a plastic pipette tip and then washed twice with PBS.¹⁵ Subsequently, the cells in one 6-well plate were infected with KGHV500, and the control group was infected with KGHV400 at the appropriate MOI. The size of the wound was determined from images captured under a microscope (Olympus, Tokyo, Japan) at 0 h, 24 h, and 36 h after wounding. The gap distance was measured, and the average length was calculated for each condition.

Transwell assay to assess cell invasion

Transwell invasion assays were carried out using a 24-well Transwell chamber as follows. Matrigel (BD Matrigel Matrix, USA) was diluted 1:20–1:30 with DMEM without FBS, and was filled in the upper compartment chamber (60 µL/well) and incubated at 37°C for 30 min. Then, cells infected by recombinant adenovirus were resuspended in serum-free DMEM and then plated in the upper wells at a concentration of 1×10^5 cells per well. The bottom chamber was filled with 600 µL of DMEM containing 10% FBS. Finally, after incubation, noninvasive cells in the top chambers were gently wiped away with a cotton swab. Invasive cells on the bottom surface of a filter were fixed with methanol, stained with Giemsa dye, and then counted under an inverted microscope (10 fields were counted for each sample).

MTT assay to assess cell viability

U251 cells were seeded in a 96-well plate at a density of 5×10^4 cells per well and cultured at 5% CO₂. When the cells reached 70% of confluence, KGHV500 was added at a MOI = 100 for infection. Then, 20 µL of an MTT solution (5 mg/mL, Amresco, USA) was added to each well at one, two, three, four, and five days after infection and further incubated at 37°C for 4 h. The supernatant was removed, and 150 µL of DMSO was added to each well and mixed for

10 min. Cell viability was determined by a microplate reader (Bio-Rad, model 680) at a wavelength of 490 nm.

TUNEL assay to assess cell apoptosis

U251 cells were collected as cell pellets at 48 h after infection with KGHV500, then, were embedded in paraffin and cut into slices. The terminal deoxynucleotidyl transferase-mediated dUTP nick end labeling (TUNEL) assay was performed with an *in situ* cell death detection kit (Roche Diagnostics GmbH, Germany) according to the kit instructions. The apoptotic cells were visualized and counted by fluorescence microscopy.

Nude mice model of U251 cell xenograft

This study received the approval of the Ethics Committee of Kunming University of Science and Technology. All animals involved in the study were cared for under institutional guidelines. The glioma xenograft tumor was established as previously described^{16,17}; 1×10^7 cells of U251 cells were injected subcutaneously in the right axilla of six-week-old female immune-deficient nude mice (Vital River Laboratories, Beijing, China). When the size of xenograft tumors reached at least 5 mm in length, CIK cells infected by recombinant adenovirus were injected into the tail veins of xenograft recipient mice for treatment. The treatment was repeated once every three days and tumor volume was measured with a caliper every day. Tumor growth curves were generated with the tumor volume calculated according to the following formula: $V = (L \times W^2)/2$.

Histology and immunohistochemistry

The nude mice were sacrificed to observe pathological lesions on every other day after treatment. Thirty-four days later, all mice were sacrificed. Xenograft tumor and organs were fixed in formalin, embedded in paraffin, sectioned at a thickness of 3–4 μm and stained with hematoxylin & eosin (H&E) for histological assessment.¹⁸ Immunohistochemistry assay was used to detect the expression of Ki67, anti-p21Ras scFv, and the adenovirus hexon protein with anti-ki67 antibody (OriGene, ZM0166, USA), anti-Flag tag mAb (Abnova, MAB9744, China), and anti-virus hexon antibody (Novus, NBP2-11638, USA), respectively.

In vivo, glioma cell proliferation was assessed by counting the percentage of Ki67 positive glioma cell nuclei. More than 1000 neoplastic cells were counted in each tumor tissue.

Western blotting

The expression of the scFv in xenografts and organs was detected by Western blotting. First, the total protein was extracted from tissues. Then, the protein samples were separated via SDS-PAGE and transferred to PVDF membranes. The membranes were incubated with anti-Flag tag monoclonal antibody (Abnova, China) overnight and then horseradish peroxidase (HRP)-conjugated secondary antibody (goat anti-mouse IgG, ZSGB-Bio, ZB-5305 China). Then, the PVDF membranes were stained with DAB, and protein

expression levels were compared with those of β -actin, an internal control. Both anti-Flag tag and HRP-conjugated secondary antibodies were used at a 1:1000 dilution.

Quantitative real-time PCR

Total RNA was extracted from tumor and organ tissues by using RNA TRIzol Reagent (East™ total RNA extraction kit, Promega, USA) according to the manufacturer's instructions. Data were collected and analyzed by Bio-Rad CFX96 Manager software. The expression level of each candidate gene was internally normalized against the expression of GAPDH.¹⁹ The relative expression levels were determined by the $2^{-\Delta\Delta\text{Ct}}$ method.

Statistical analysis

The experiment was performed in triplicate for each group, and the results were averaged. Values are expressed as the mean \pm SD. SPSS 22.0 software was used for statistical analyses. Comparisons among groups were analyzed using one-way ANOVA followed by LSD-t test. The statistical significance of differences between the control and treatment groups was calculated, and differences for which the *P*-value < 0.05 were considered statistically significant.

Results

U251 cells and CIK cells infection by the recombinant adenoviruses

Human glioblastoma cell line U251 presented malignant pathological characteristics such as large cell size, irregular morphology, large nuclei, hyperchromatic nuclei and a high nucleus-to-cytoplasm ratio, and a high expression of CD46 protein on the surface of the cells. CD46 is the receptor of fiber 35 proteins, allowing U251 cells to bind to KGHV500 and KGHV400. We found that U251 cells overexpressed p21H-Ras, which led them to be the target of anti-p21Ras scFv. After co-cultured with KGHV500, many virus particles at a diameter of 70–100 nm were found in the cytoplasm and cell nucleus of U251 cells under electron (Figure 1(A)). TCID50 assay revealed that the highest KGHV500 infection efficiency was an MOI of 100 (Figure 1(B)).

We prepared CIK cells from PBMCs by a combined treatment with IFN- γ , IL-1 α , and IL-2 for 14 days as described in the Materials and methods. The isolated cells were identified by immunohistochemistry and showed the phenotypic characteristics of CIK cells, that is, CD3⁺ and CD56⁺. These data suggested that the PBMCs cells had been successfully induced to CIK cells. Moreover, similar to the adenovirus CD46 receptor on the U251 cell membrane, nearly all the CIK cells expressed CD46 protein on the cell surface. After co-culture with KGHV500 or KGHV400, the hexon protein was detected in all CIK cells, which means that CIK cells could interact with adenovirus due to the expression of the CD46 receptor (Figure 1(C)).

Anti-tumor efficacy of KGHV500 in vitro

We performed a scratch test after U251 cells were infected with KGHV500 at MOI = 100 to investigate migration

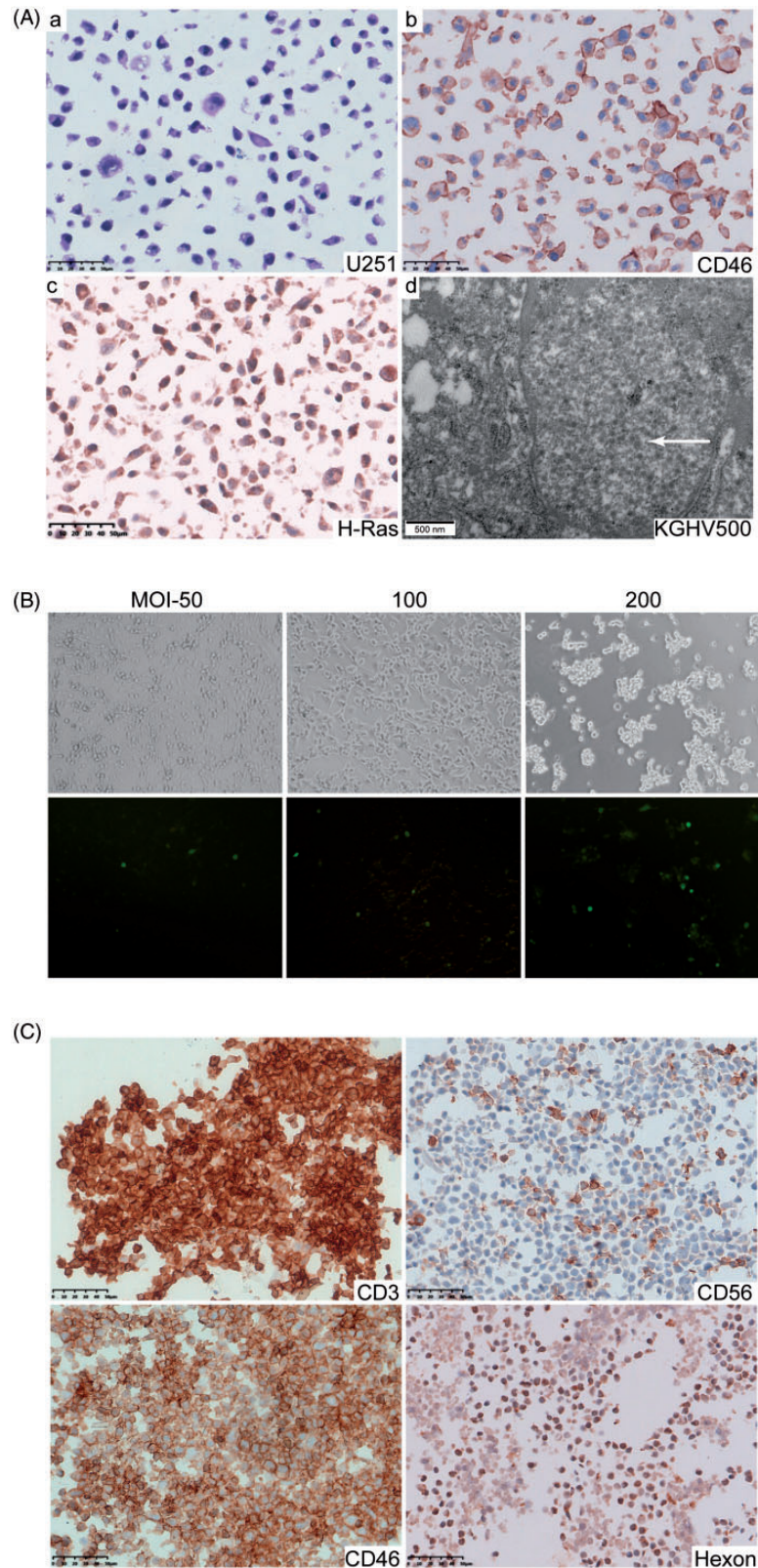


Figure 1. U251 cells and CIK cells were infected by recombinant adenovirus KGHV500. (A) (a) U251 cells presented the following malignant pathological characteristics: large cell size, irregular morphology, large nuclei, hyperchromatic nuclei, and a high nucleus-to-cytoplasm ratio (H&E staining). (b) CD46, the receptor of KGHV500 fiber proteins, was highly expressed on the surface of U251 cells (IHC staining). (c) H-p21Ras was overexpressed in the cytoplasm of U251 cells (IHC staining). (d) Many KGHV500 viral particles with a diameter of 70–100 nm were observed in the cytoplasm and nuclei of U251 cells by electron microscopy (arrow). Scale bars = 50 μ m and 500 nm, respectively. (B) The KGHV500 virus infection efficiency in U251 cells was detected by calculating the TCID₅₀. The best infection efficiency was achieved at an MOI of 100, at which the strongest fluorescence signal and weakest cytopathic effect were observed. (C) The IHC staining showed that CIK markers CD3, CD56 were expressed on the cell membrane. CD46 protein, the adenovirus receptor, was clearly expressed on the surface of CIK cells. The adenovirus hexon protein was detected in CIK cells after their infection with KGHV500. (A color version of this figure is available in the online journal.)

ability of cells. At 24 h and 36 h after infection, the wound healing area was smaller in the KGHV500 group than that in the KGHV400 group and the uninfected group ($P < 0.01$) (Figure 2(a) and (b)). Transwell invasion assays were used

to detect whether KGHV500 could inhibit tumor invasion. The results showed that the number of U251 cells that invaded the bottom chamber reduced significantly in the KGHV500 group compared with the KGHV400 group (P

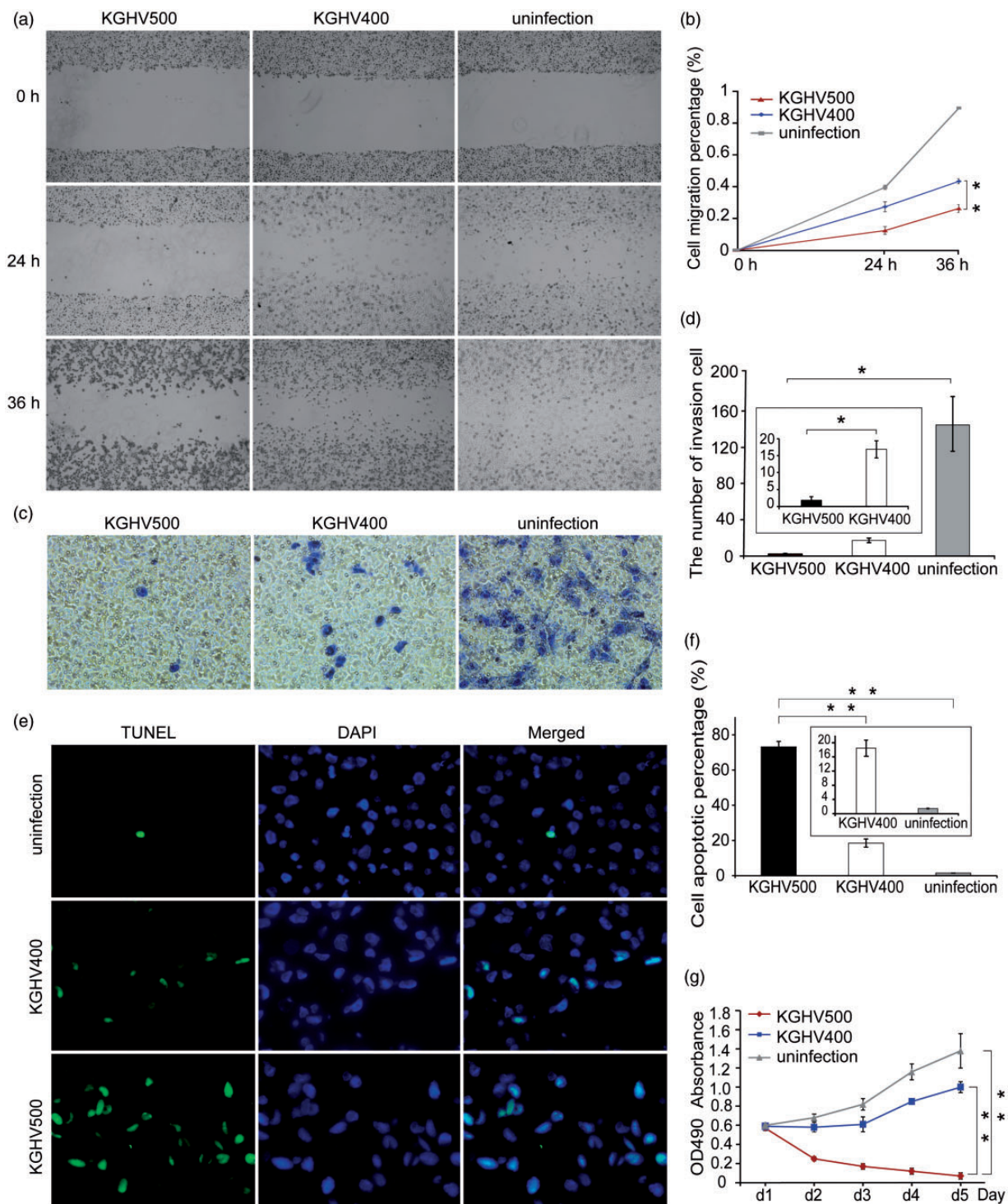


Figure 2. The anti-tumor efficacy of KGHV500 *in vitro*. (a, b) Cell migration was measured by scratch test at 0 h, 24 h, and 36 h after U251 cells were infected with KGHV500. The migration of U251 cells was inhibited by KGHV500 and KGHV400, and the extent of this inhibition was greater in the KGHV500 group than in the KGHV400 group. (c, d) Transwell invasion assays showed that the invasion ability of U251 cells was decreased in the KGHV500 group compared to the KGHV400 and PBS groups. (e, f) U251 cell apoptosis after viral infection was detected by TUNEL assays. The percentage of apoptotic cells in the KGHV500 group was higher than that in the KGHV400 and PBS groups. (g) U251 cell proliferation was tested by MTT assay at 1 d, 2 d, 3 d, 4 d, and 5 d after infection with KGHV500. Among the three groups, proliferation was lowest in U251 cells infected with KGHV500. All experiments were performed in triplicate. All the data are represented as the means \pm standard deviation (SD) of three experiments. * $P < 0.05$; ** $P < 0.01$. (A color version of this figure is available in the online journal.)

<0.05) (Figure 2(c) and (d)). In TUNEL assay, an increased proportion of apoptotic U251 cells was observed in the KGHV500 group compared with the KGHV400 control group ($73.10 \pm 3.14\%$ vs. $18.46 \pm 2.32\%$, $P < 0.01$) (Figure 2(e)). However, only a few apoptotic cells were observed in the uninfected group (Figure 2(f)). As a result, the recombinant adenovirus KGHV500 induced a significant degree of U251 cell death via apoptosis. After infection with the virus KGHV500, an MTT assay was employed to determine whether KGHV500 could inhibit the proliferation activity of U251 cells. As shown in Figure 2(g), on the first day, the number of living U251 cells of the three groups was almost the same. However, on the fifth day, the number of living cells in the KGHV500-infected group decreased sharply compared with KGHV400-infected group and the uninfected group. The number of living U251 cells in the KGHV400-infected group was 16 times higher than that in the KGHV500-infected group, and the number of living U251 cells in the uninfected group was 22 times higher than that in the KGHV500-infected group.

In vivo anti-tumor efficacy of KGHV500

We established a U251 xenograft model in nude mice and administered CIK cells carrying KGHV500 to treat the mice through tail vein injection. Tumor growth curves were drawn according to the tumor volume (Figure 3(a) and (b)). From tumor growth curves, the slowest tumor growth was observed in the CIK+KGHV500 group, in contrast to the fastest tumor growth observed in the PBS group. The pace of growth in CIK, KGHV500, CIK+KGHV400 groups is decreased ($P < 0.01$). These results indicated that KGHV500 delivered by CIK cells could obviously suppress the tumor growth *in vivo*, and its anti-tumor effect was better than other groups. Ki67 proliferation index revealed a reduced tumor cell proliferation in CIK+KGHV500 treatment compared to the CIK+KGHV400 ($16.33 \pm 1.53\%$ vs. $28 \pm 4.36\%$, $P < 0.05$) and KGHV500 group ($16.33 \pm 1.53\%$ vs. $37 \pm 7\%$, $P < 0.01$) as well as other groups ($P < 0.01$) in tumor tissue (Figure 3(c) and (e)). Then, we performed TUNEL staining on tumor tissue sections to assess whether KGHV500 could lead to apoptosis *in vivo* (Figure 3(d) and (e)). We observed more apoptotic cells in CIK+KGHV500 group (78.20 ± 3.52) % compared with the CIK+KGHV400 groups (27.23 ± 3.21) % and other groups ($P < 0.01$). There was almost no apoptosis cell in the PBS group (2.10 ± 0.99) %, which was the same result as what was observed *in vitro*. These results implied that the CIK+KGHV500 has the ability to inhibit proliferation and induce the apoptosis of U251 cells *in vivo*. Further, the expression of apoptosis-associated genes was detected by real-time PCR (qPCR). As a result, the expression of proapoptotic genes (Caspase-3, Caspase-7, and p53) was upregulated, while the expression of antiapoptotic genes (Bcl-2 and Survivin) was downregulated in the CIK+KGHV500 group (Figure 3(f)). Real-time PCR (qPCR) verified the TUNEL assay results and revealed the cause of apoptosis at the gene level.

KGHV500 and anti-p21Ras scFv in tumors and major organs

To determine whether CIK cells delivered KGHV500 to the transplanted tumors, we still needed to confirm these tumors truly expressed anti-p21Ras scFv *in vivo*. The nude mice from each group were sacrificed on days 1, 3, 5, and 7 after treatment, and the tumors and 10 major organs including heart, liver, spleen, lung, kidney, stomach, pancreas, brain, small intestine, large intestine were removed. No significant pathological lesions were found in organs of the nude mice in both experimental and control groups. Adenovirus hexon protein and anti-p21Ras scFv were detected in the tumor by immunohistochemistry. From day 1, the tumor began to express hexon protein in both CIK+KGHV500 experimental group and KGHV500 group. As time progressed, we also found that the hexon expression increased gradually in both groups. The CIK+KGHV500 experimental group expressed more scFv in the tumor than did the KGHV500 group. A significant difference was found between the two groups ($P < 0.05$) (Figure 4(a) and (b)). Correspondingly, we found that xenograft tumors from the CIK+KGHV500 group expressed more anti-p21Ras scFv than xenograft tumors from the KGHV500 group ($P < 0.05$) (Figure 4(c) and (d)). These results indicated that the CIK+KGHV500 group could target the tumor.

To observe the safety of KGHV500 in the body, we analyzed the hexon and anti-p21Ras scFv distribution in organs. In the KGHV500 group, adenovirus hexon was expressed in all of the above organs except the brain, while we observed the positive hexon expression only in the liver, spleen, and kidney in CIK+KGHV500 group (Figure 5(a)). These results indicated that the toxicity of CIK combined with KGHV500 delivery through the blood in the nude mouse model was decreased.

We further performed Western blotting to detect the expression of scFv in the tumors and major organs. The data showed strong expression of scFv in tumors but little scFv expression in the liver, kidney, and spleen of mice in the CIK+KGHV500 group (Figure 5(b)). In the KGHV500 group, scFv expression was detected in all tested organs except for the brain (Figure 5(c)).

Discussion

Human glioblastoma cell line U251 was established at the Wallenberg laboratory, Uppsala, Sweden in the 1960s and was derived from a male patient with malignant astrocytoma.²⁰ Since U251 cells present a high expression of p21Ras protein, we may take it as a target and carry out treatment experiments using anti-p21Ras scFv to explore a new treatment method for glioma. Here, we found that recombinant adenovirus KGHV500 harboring anti-p21Ras scFv gene could infect U251 cells, then proliferate and express the scFv intracellularly. Consequently, the proliferation and migration of U251 cells were inhibited, resulting in more apoptosis. *In vivo*, CIK cells successfully delivered KGHV500 to the U251 cell xenografts through the blood. Then, KGHV500 expressed anti-p21Ras scFv and repressed tumor growth significantly. Moreover, we also found that

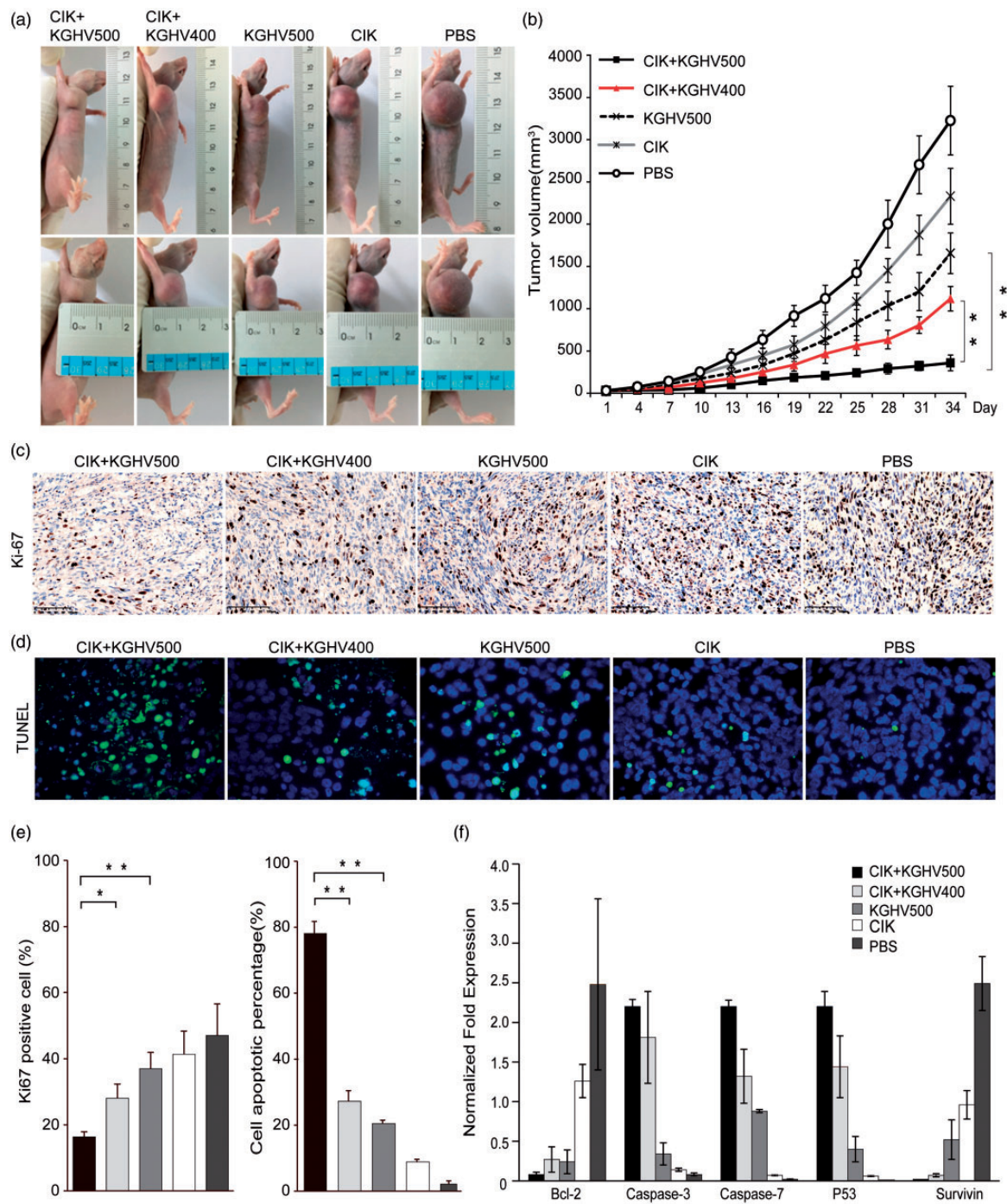


Figure 3. *In vivo* anti-tumor efficacy against human glioma cell line xenografts. (a, b) U251 cells were subcutaneously inoculated into the right axillae of BALB/c nude mice to establish a xenograft model, and CIK cells carrying recombinant adenovirus were injected by the tail vein. Tumor growth curves were drawn according to the tumor volume. Tumor volumes in the different groups increased in the following order: the CIK + KGHV500, CIK + KGHV400, KGHV500, CIK, and PBS groups. Means \pm SD. (c) Cell proliferation of xenograft tumor was visualized by IHC of Ki67 proliferation index. The expression of Ki67 was showed the dark brown color with cell nuclei. Scale bars = 100 μ m (d) TUNEL staining (green fluorescence) was observed in the cytoplasm of apoptotic cells, and cell nuclei were stained with DAPI (blue fluorescence). (e) The bars show quantitative analysis of the Ki67 positive cells and the TUNEL staining in all groups. The Ki67 was apparently reduced in CIK + KGHV500 group than other groups after treatment. There were more apoptotic tumor cells in the CIK + KGHV500 group than in the other four groups. (f) qPCR analysis revealed that expression of the proapoptotic genes Caspase-3, Caspase-7, and p53 was upregulated, while expression of the antiapoptotic genes Bcl-2 and Survivin was downregulated in the KGHV500 + CIK group. Means \pm SD. * P < 0.05; ** P < 0.01. (A color version of this figure is available in the online journal.)

the KGHV500 promoted the apoptosis of U251 cells by upregulating the Caspase-3, Caspase-7, and p53 genes while downregulating the Bcl-2 and Survivin genes.

Gene therapy has broadened the concept with the introduction of "therapeutic" genes to cells in the 1970s²¹ and is

regarded as a powerful tool to regulate biological functions in diseased tissues and to treat cancers.²² The use of a suitable vector is essential for successful gene treatment. Adenovirus (Ad), the most commonly used vector, has significant advantages of gene delivery due to its relative ease

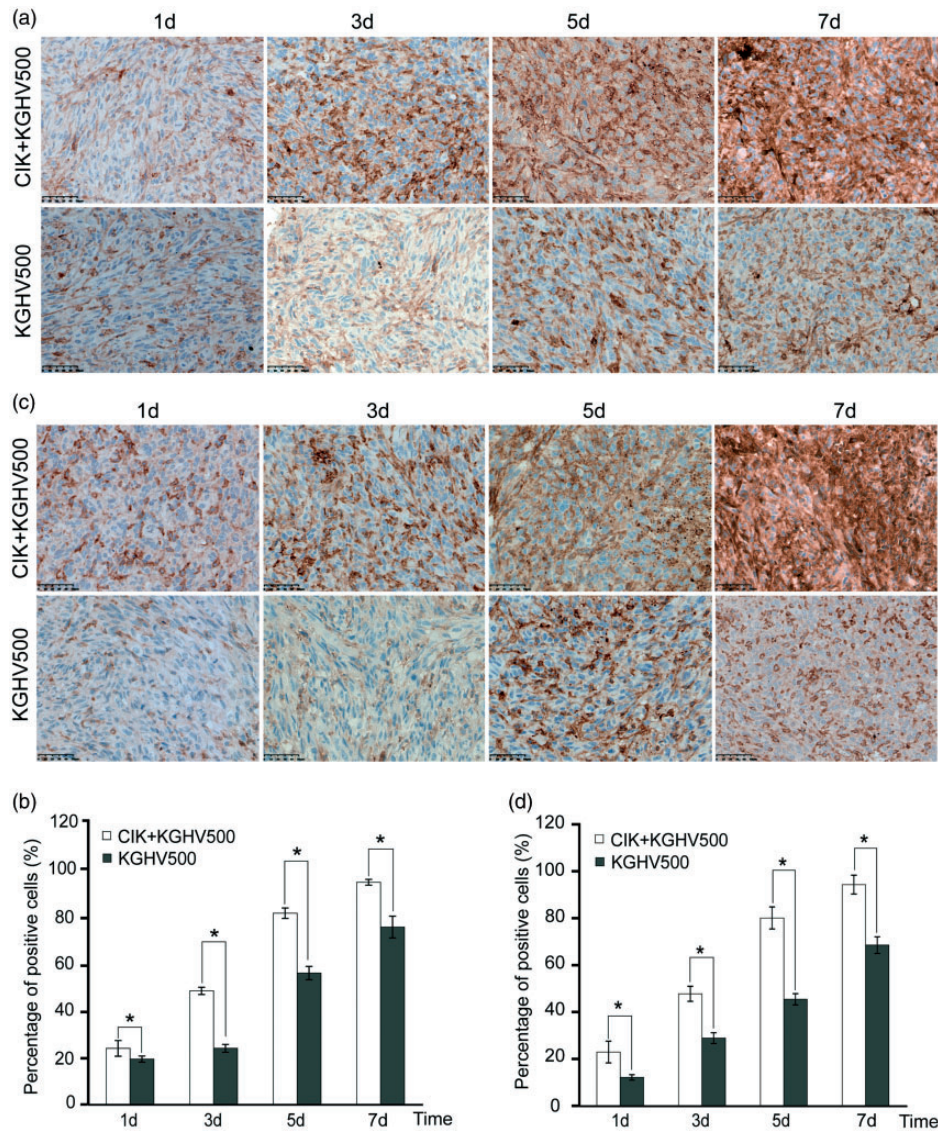


Figure 4. Expression of the adenovirus nucleocapsid protein (Hexon) and anti-p21-Ras scFv in tumors was examined by immunohistochemistry. (a, b) The expression of hexon increased gradually from the first day to the 7th day, and hexon expression was higher in the CIK+KGHV500 group than in the KGHV500 group on the same days. (c, d) The expression of anti-p21-Ras scFv in the tumors. The CIK+KGHV500 group expressed more anti-p21-Ras scFv than the KGHV500 group on the same days. Scale bars = 50 μ m. Means \pm SD. * $P < 0.05$; ** $P < 0.01$. (A color version of this figure is available in the online journal.)

of modification, ability to purify high titers, high efficiency of transgene expression, and stable gene transfer into many different tissue types. In this study, the recombinant adenovirus KGHV500 was derived from wild-type adenovirus 5 (Ad5). In KGHV500, the E1A promoter of Ad5 was replaced with the human telomerase reverse transcriptase (hTERT) promoter, and the E1B promoter was replaced with the hypoxia response element (HRE) promoter, which gave KGHV500 the ability to specific replicate in tumor cells. Besides, the fiber gene of Ad5 was replaced with the adenovirus 35, which allowed KGHV500 to bind the CD46 on the surface of CIK cells. Moreover, as glioma cells are resistant to Ad5 infection due to their low coxsackie-adenovirus receptor (CAR) expression,²³⁻²⁵ we use recombinant adenovirus KGHV500 as a vector that has the ability to bind CD46 protein to enhance the gene transduction efficiency.

Some researchers reported that CIK cells could inhibit the growth of GBM in intratumoral injection or intravenous injection.^{14,18} Those mainly relied on CIK cells to harbor the non-major histocompatibility complex-restricted cytotoxicity of natural killer cells and T cell anti-tumor activity.²⁶ Here, we utilized CIK cells to successfully deliver KGHV500 to the tumor site²⁷ as CIK cells are immune cells and thus can recognize NKG2D ligands on the tumor surface²⁸ as well as exhibit tumor-specific tropism. Moreover, this method can avoid clearance and a decrease in the level of circulating viral particles by neutralizing antibodies.^{29,30} Thorne *et al.*²⁷ first reported the use of CIK cells to carry the vaccinia virus to cancer, where it killed tumor cells. Yang *et al.*³¹ recently employed CIK cells to carry oncolytic adenovirus as a combined therapy for liver cancer. Both of them obtained satisfactory results. In our study, since CIK cells were used as the drug carrier,

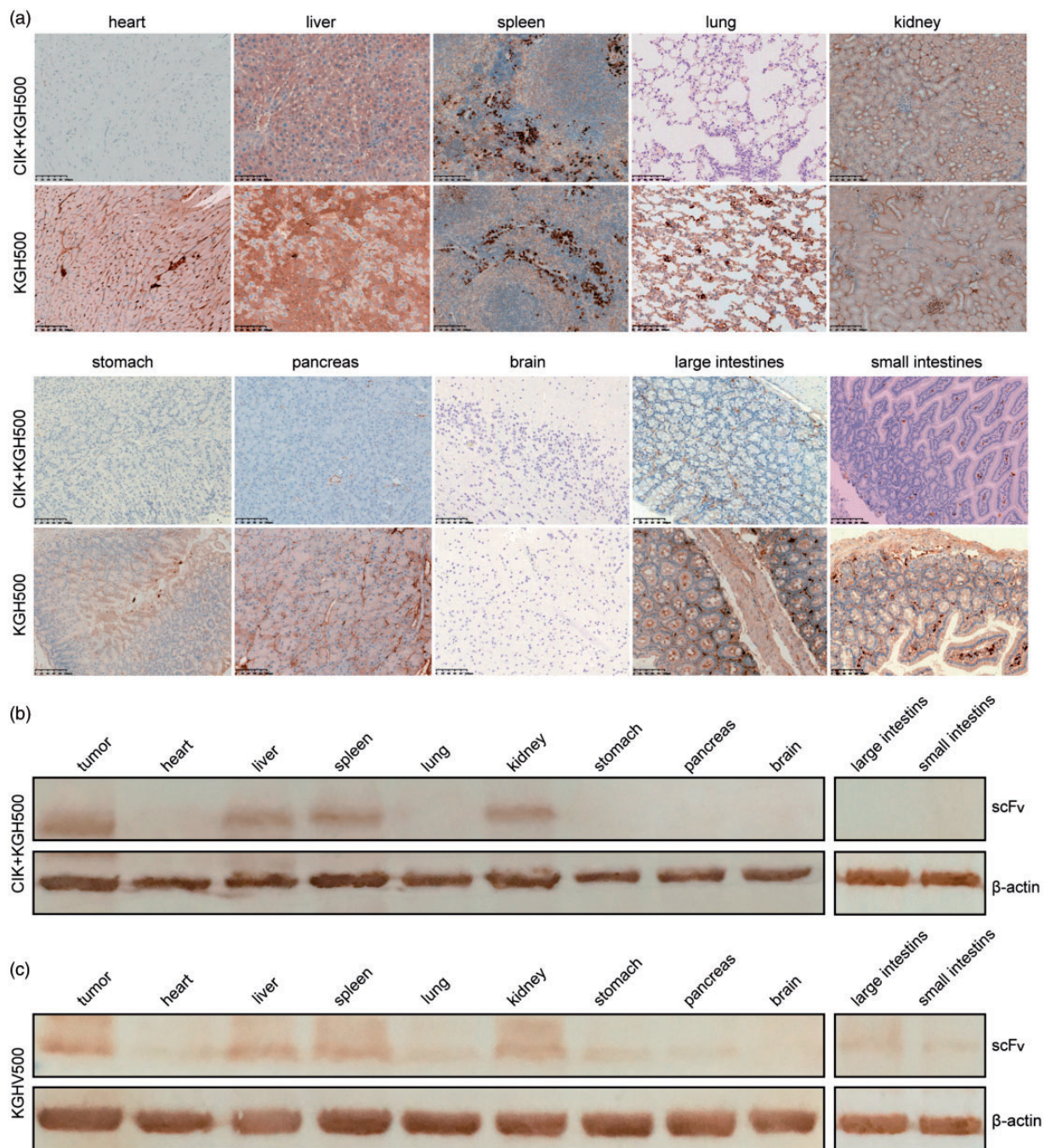


Figure 5. The expression of hexon and anti-p21 Ras scFv in the major organs of nude mice. (a) Hexon was detected by immunostaining in all tested organs except for the brain in the KGVH500 group. However, in the CIK+KGVH500 group, only the liver, spleen, kidney, and tumor exhibited detectable hexon levels. Scale bars = 100 μ m. (b, c). Western blotting showed that anti-p21-Ras scFv was expressed in only tumors and the liver, spleen, and kidney in the CIK+KGVH500 group. In contrast, the scFv was expressed in tumors and all tissues except for the brain in the KGVH500 group. (A color version of this figure is available in the online journal.)

the injected number of CIK cells was lower than that of therapeutic use. That might be a reason to explain the ability to inhibit tumor growth in the CIK group was weakened than the KGVH500 group. Since CIK cells can protect the viral vector from host immunosurveillance and deliver the vector to distant tumor regions, our study also expands evidence that CIK could be a promising second drug carrier.

In virus-based gene therapy, systematic administration generally leads to unwanted vector uptake by many

different cell types in multiple organs.³² In addition to target specificity, obtaining a safe method of systemic administration is an important goal that must be met. In the present study, compared with the KGVH500 group, most tissues in the CIK + KGVH500 groups exhibited almost no adenovirus hexon and anti-p21 Ras scFv expression, but small amounts of these proteins were detected in the livers, spleens, and kidneys of mice in the CIK + KGVH500 group. Other researchers reported a low level of Ad5/F35 adenovirus expression in the human

liver³³ and monkey liver.³⁴ Ad5/F35 might enable a small degree of nonparenchymal liver cell infection but not parenchymal liver cell infection.³⁵ The low level of Ad5/F35 expression in the spleen might be related to the homing of CIK cells to peripheral lymphoid organs.³⁶ We assume that KGHV500 and scFv could be detected in the kidneys in both the experimental and control groups because the kidneys are excretory organs.

Furthermore, KGHV500 infects cells by binding its fiber35 protein to the CD46 molecule, the receptor for fiber35, on the cell surface, including CIK cells, dendritic cells³⁷ human hematopoietic progenitor cells,³⁸ and epithelial cells³⁹ and fibroblasts.⁴⁰ KGHV500 is regulated by two tumor-specific promoters hTERT and HRE. Therefore, it replicates and continuously expresses anti-p21 Ras scFv in tumor cells but does not replicate and proliferate in normal cells. Although it can infect some normal cells with CD46, it only expresses anti-p21 Ras scFv briefly. This is why the hexon and anti-p21Ras scFv were observed in the liver, kidney, spleen, and other organs, but no cell damage was observed under pathological examination.

As reported in some studies, p21Ras was expressed in embryonic cells and a few normal adult cells.³ These normal adult cells might be infected by KGHV500 if they express CD46. However, the impact on Ras function should be very small since KGHV500 does not replicate in the cells. More importantly, in this study, CIK cells with tumor-targeting were used to deliver KGHV500 to transplanted tumors through blood *in vivo*, which largely avoided the infection of normal cells on the way.

In summary, the present study demonstrates that recombinant adenovirus KGHV500 could intracellularly express anti-p21Ras scFv in human glioma cell line U251, then inhibit U251 cell growth, migration, and invasion; and promoted glioma cell apoptosis. *In vivo*, CIK cells could deliver KGHV500 to glioma xenografts in nude mice with relative safety. Our findings expand evidence that targeting Ras is a useful therapeutic strategy for gliomas and other Ras-driven cancers. We believe that anti-p21Ras scFv delivered by recombinant adenovirus and CIK cells may play an essential role in the therapy of Ras-driven cancers.

AUTHORS' CONTRIBUTIONS

Conceptualization, JLY and MY; Investigation, MY, LLY; Resources, QF and XYP; Writing—Original Draft, JQ; Supervision, XYP, QF, and JLY; Funding Acquisitions, JLY. All authors read and approved the final manuscript.

DECLARATION OF CONFLICTING INTERESTS

The author(s) declared no potential conflicts of interest with respect to the research, authorship, and/or publication of this article.

FUNDING

The author(s) disclosed receipt of the following financial support for the research, authorship, and/or publication of this article: This work was supported by the National Natural Science Foundation of China [81460464]; and the Major

Science and Technology Project of the Yunnan Science and Technology Plan [2018ZF009].

ORCID iD

Ju-Lun Yang  <https://orcid.org/0000-0002-0934-5238>

REFERENCES

1. Ferlay J, Soerjomataram I, Dikshit R, Eser S, Mathers C, Rebelo M, Parkin DM, Forman D, Bray F. Cancer incidence and mortality worldwide: sources, methods and major patterns in GLOBOCAN 2012. *Int J Cancer* 2015;**136**:E359–86
2. Stupp R, Mason WP, van den Bent MJ, Weller M, Fisher B, Taphoorn MJ, Belanger K, Brandes AA, Marosi C, Bogdahn U, Curschmann J, Janzer RC, Ludwin SK, Gorlia T, Allgeier A, Lacombe D, Cairncross JG, Eisenhauer E, Mirimanoff RO. Radiotherapy plus concomitant and adjuvant temozolomide for glioblastoma. *N Engl J Med* 2005;**352**:987–96
3. Barbacid M. Ras genes. *Annu Rev Biochem* 1987;**56**:779–827
4. Fernandez-Medarde A, Santos E. Ras in cancer and developmental diseases. *Genes Cancer* 2011;**2**:344–58
5. Gerosa MA, Talarico D, Fognani C, Raimondi E, Colombatti M, Tridente G, De Carli L, Della Valle G. Overexpression of N-ras oncogene and epidermal growth factor receptor gene in human glioblastomas. *J Natl Cancer Inst* 1989;**81**:63–7
6. Lymbouridou R, Soufla G, Chatzinikola AM, Vakis A, Spandidos DA. Down-regulation of K-ras and H-ras in human brain gliomas. *Eur J Cancer* 2009;**45**:1294–303
7. Prigent SA, Nagane M, Lin H, Huvar I, Boss GR, Feramisco JR, Cavenee WK, Huang HS. Enhanced tumorigenic behavior of glioblastoma cells expressing a truncated epidermal growth factor receptor is mediated through the Ras-Shc-Grb2 pathway. *J Biol Chem* 1996;**271**:25639–45
8. Knobbe CB, Reifemberger J, Reifemberger G. Mutation analysis of the ras pathway genes NRAS, HRAS, KRAS and BRAF in glioblastomas. *Acta Neuropathol* 2004;**108**:467–70
9. Cancer genome atlas research N. Comprehensive genomic characterization defines human glioblastoma genes and core pathways. *Nature* 2008;**455**:1061–8
10. Lin XR, Zhou XL, Feng Q, Pan XY, Song SL, Fang H, Lei J, Yang JL. CIK cell-based delivery of recombinant adenovirus KGHV500 carrying the anti-p21Ras scFv gene enhances the anti-tumor effect and safety in lung cancer. *J Cancer Res Clin Oncol* 2019;**145**:1123–32
11. Liu FR, Bai S, Feng Q, Pan XY, Song SL, Fang H, Cui J, Yang JL. Anticancer effects of anti-p21Ras scFv delivered by the recombinant adenovirus KGHV500 and cytokine-induced killer cells. *BMC Cancer* 2018;**18**:1087
12. Wang M, Hong Y, Feng Q, Pan X, Song S, Cui J, Lei J, Fang H, Yang J. Recombinant adenovirus KGHV500 and CIK cells codeliver anti-p21-Ras scFv for the treatment of gastric cancer with Wild-Type ras overexpression. *Mol Ther Oncolytics* 2018;**11**:90–101
13. Hallenbeck PL, Chang YN, Hay C, Golightly D, Stewart D, Lin J, Phipps S, Chiang YL. A novel tumor-specific replication-restricted adenoviral vector for gene therapy of hepatocellular carcinoma. *Hum Gene Ther* 1999;**10**:1721–33
14. Kim HM, Kang JS, Lim J, Kim JY, Kim YJ, Lee SJ, Song S, Hong JT, Kim Y, Han SB. Antitumor activity of cytokine-induced killer cells in nude mouse xenograft model. *Arch Pharm Res* 2009;**32**:781–7
15. Wu H, Li X, Feng M, Yao L, Deng Z, Zao G, Zhou Y, Chen S, Du Z. Downregulation of RNF138 inhibits cellular proliferation, migration, invasion and EMT in glioma cells via suppression of the ERK signaling pathway. *Oncol Rep* 2018;**40**:3285–96
16. Cao WQ, Li Y, Hou YJ, Yang MX, Fu XQ, Zhao BS, Jiang HM, Fu XY. Enhanced anticancer efficiency of doxorubicin against human glioma by natural borneol through triggering ROS-mediated signal. *Biomed Pharmacother* 2019;**118**:109261
17. Diao Y, Jin B, Huang L, Zhou W. MiR-129-5p inhibits glioma cell progression in vitro and in vivo by targeting TGIF2. *J Cell Mol Med* 2018;**22**:2357–67

18. Wang P, Yu JP, Gao SY, An XM, Ren XB, Wang XG, Li WL. Experimental study on the treatment of intracerebral glioma xenograft with human cytokine-induced killer cells. *Cell Immunol* 2008;**253**:59–65
19. Cui F, Wu D, He X, Wang W, Xi J, Wang M. Long noncoding RNA SPRY4-IT1 promotes esophageal squamous cell carcinoma cell proliferation, invasion, and epithelial-mesenchymal transition. *Tumour Biol* 2016;**37**:10871–6
20. Torsvik A, Stieber D, Enger PØ, Golebiewska A, Molven A, Svendsen A, Westermark B, Niclou SP, Olsen TK, Chekenya Enger M, Bjerkvig R. U-251 revisited: genetic drift and phenotypic consequences of long-term cultures of glioblastoma cells. *Cancer Med* 2014;**3**:812–24
21. Friedmann T, Roblin R. Gene therapy for human genetic disease? *Science* 1972;**175**:949–55
22. Alexander BL, Ali RR, Alton EW, Bainbridge JW, Braun S, Cheng SH, Flotte TR, Gaspar HB, Grez M, Griesenbach U, Kaplitt MG, Ott MG, Seger R, Simons M, Thrasher AJ, Thrasher AZ, Yla-Herttuala S. Progress and prospects: gene therapy clinical trials (part 1). *Gene Ther* 2007;**14**:1439–47
23. Nandi S, Lesniak MS. Adenoviral virotherapy for malignant brain tumors. *Expert Opin Biol Ther* 2009;**9**:737–47
24. Asaoka K, Tada M, Sawamura Y, Ikeda J, Abe H. Dependence of efficient adenoviral gene delivery in malignant glioma cells on the expression levels of the coxsackievirus and adenovirus receptor. *J Neurosurg* 2000;**92**:1002–8
25. Huang KC, Altinoz M, Wosik K, Larochelle N, Koty Z, Zhu L, Holland PC, Nalbantoglu J. Impact of the coxsackie and adenovirus receptor (CAR) on glioma cell growth and invasion: requirement for the C-terminal domain. *Int J Cancer* 2005;**113**:738–45
26. Zhang J, Zhu L, Zhang Q, He X, Yin Y, Gu Y, Guo R, Lu K, Liu L, Liu P, Shu Y. Effects of cytokine-induced killer cell treatment in colorectal cancer patients: a retrospective study. *Biomed Pharmacother* 2014;**68**:715–20
27. Thorne SH, Negrin RS, Contag CH. Synergistic antitumor effects of immune cell-viral biotherapy. *Science* 2006;**311**:1780–4
28. Verneris MR, Karimi M, Baker J, Jayaswal A, Negrin RS. Role of NKG2D signaling in the cytotoxicity of activated and expanded CD8+ T cells. *Blood* 2004;**103**:3065–72
29. Yamamoto M, Curiel DT. Current issues and future directions of oncolytic adenoviruses. *Mol Ther* 2010;**18**:243–50
30. Alemany R, Suzuki K, Curiel DT. Blood clearance rates of adenovirus type 5 in mice. *J Gen Virol* 2000;**81**:2605–9
31. Yang Z, Zhang Q, Xu K, Shan J, Shen J, Liu L, Xu Y, Xia F, Bie P, Zhang X, Cui Y, Bian XW, Qian C. Combined therapy with cytokine-induced killer cells and oncolytic adenovirus expressing IL-12 induce enhanced antitumor activity in liver tumor model. *PLoS One* 2012;**7**:e44802
32. Thomas CE, Ehrhardt A, Kay MA. Progress and problems with the use of viral vectors for gene therapy. *Nat Rev Genet* 2003;**4**:346–58
33. Cho YS, Do MH, Kwon SY, Moon C, Kim K, Lee K, Lee SJ, Hemmi S, Joo YE, Kim MS, Jung C. Efficacy of CD46-targeting chimeric Ad5/35 adenoviral gene therapy for colorectal cancers. *Oncotarget* 2016;**7**:38210–23
34. Xin KQ, Jounai N, Someya K, Honma K, Mizuguchi H, Naganawa S, Kitamura K, Hayakawa T, Saha S, Takeshita F, Okuda K, Honda M, Klinman DM, Okuda K. Prime-boost vaccination with plasmid DNA and a chimeric adenovirus type 5 vector with type 35 fiber induces protective immunity against HIV. *Gene Ther* 2005;**12**:1769–77
35. Sakurai F, Mizuguchi H, Yamaguchi T, Hayakawa T. Characterization of in vitro and in vivo gene transfer properties of adenovirus serotype 35 vector. *Mol Ther* 2003;**8**:813–21
36. Wang H, Cao F, Li J, Li Y, Liu X, Wang L, Liu Z, Li Y, Zhao H, Zhou J. Homing of cytokine-induced killer cells during the treatment of acute promyelocytic leukemia. *Int J Hematol* 2014;**100**:165–70
37. Sakurai F, Nakashima K, Yamaguchi T, Ichinose T, Kawabata K, Hayakawa T, Mizuguchi H. Adenovirus serotype 35 vector-induced innate immune responses in dendritic cells derived from wild-type and human CD46-transgenic mice: COMPARISON with a fiber-substituted ad vector containing fiber proteins of ad serotype 35. *J Control Release* 2010;**148**:212–8
38. Yotnda P, Onishi H, Heslop HE, Shayakhmetov D, Lieber A, Brenner M, Davis A. Efficient infection of primitive hematopoietic stem cells by modified adenovirus. *Gene Ther* 2001;**8**:930–7
39. Li K, Feito MJ, Sacks SH, Sheerin NS. CD46 (membrane cofactor protein) acts as a human epithelial cell receptor for internalization of opsonized uropathogenic *Escherichia coli*. *J Immunol* 2006;**177**:2543–51
40. Yu L, Shimozato O, Li Q, Kawamura K, Ma G, Namba M, Ogawa T, Kaiho I, Tagawa M. Adenovirus type 5 substituted with type 11 or 35 fiber structure increases its infectivity to human cells enabling dual gene transfer in CD46-dependent and -independent manners. *Anticancer Res* 2007;**27**:2311–6

(Received October 21, 2020, Accepted December 17, 2020)